Enhancement of the phase separation aspect in the electron doped manganite $Ca_{0.8}Sm_{0.16}Nd_{0.04}MnO_3$

2003 J. Phys.: Condens. Matter 15 8351

(http://iopscience.iop.org/0953-8984/15/49/013)

INSTITUTE OF PHYSICS PUBLISHING JOURNAL OF PHYSICS: CONDENSED MATTER

J. Phys.: Condens. Matter **15** (2003) 8351–8361 PII: S0953-8984(03)68146-4

Enhancement of the phase separation aspect in the electron doped manganite $Ca_{0.8}Sm_{0.16}Nd_{0.04}MnO_3$

D A Filippov[1], K V Klimov[1], R Z Levitin[1], A N Vasil'ev[1], T N Voloshok[1] and R Suryanarayanan[2,3]

[1] Physics Faculty, Moscow State University, 119992, Moscow, Russia
[2] Laboratoire de Physico-Chimie de l'Etat Solide, Bâtiment 414 Université Paris-Sud UMR 8648, 91405 Orsay, France

E-mail: ramanathan.suryan@lpces.u-psud.fr

Received 26 August 2003, in final form 15 October 2003
Published 25 November 2003
Online at stacks.iop.org/JPhysCM/15/8351

Abstract

The complex lanthanide doping of electron manganites results in enhancement of various phase separation effects in physical properties of these compounds. Selecting $Ca_{0.8}Sm_{0.16}Nd_{0.04}MnO_3$ as a model case we show that the first order structural phase transition from the paramagnetic semi-metallic phase into the anti-ferromagnetic semi-metallic phase at $T_S \sim 158 \pm 4$ K is marked by an abrupt decrease in magnetization, a steplike anomaly $\Delta L/L = 10^{-4}$ in the thermal expansion and a large latent heat $\Delta Q = 610$ J mol^{-1}. In a certain temperature range below T_S, the high field magnetization exhibits hysteretic metamagnetic behaviour due to a field induced first order transformation. The temperature dependences of ac susceptibility, magnetization and resistivity suggest rather a non-uniform state in $Ca_{0.8}Sm_{0.16}Nd_{0.04}MnO_3$ at low temperatures. The metal–insulator transition occurs at $T_{MI} \sim 112 \pm 3$ K, accompanied by a steplike increase in magnetization. These features could be ascribed to 'sponging' of electrons from the neighbouring anti-ferromagnetic matrix by clusters undergoing the ferromagnetic ordering. The spontaneous magnetization of $Ca_{0.8}Sm_{0.16}Nd_{0.04}MnO_3$ at low temperatures is about 0.1% of the calculated saturation magnetization for this compound.

1. Introduction

Some of the several factors of primary importance influencing the physical properties of the well known colossal magnetoresistance manganite perovskites $A_{1-x}D_xMnO_3$ are the ratio of Mn^{3+}/Mn^{4+} ions, the sizes of divalent (D) to trivalent cations (A) substituted at the A site of the perovskite structure and the spread in sizes of these cations [1, 2]. The ratio of trivalent and tetravalent manganese ions defines the carrier density. This quantity is of key importance in

[3] Author to whom any correspondence should be addressed.

the determination of competition of insulating anti-ferromagnetic and metallic ferromagnetic states. The lengths and angles of Mn–O–Mn bonds in the perovskite structure are determined by the size of A cations, while the variance in their sizes is related to disorder effects in these systems [3]. The disorder effects have led to the understanding that the manganite perovskites are intrinsically non-uniform systems [4, 5]. There is manifold evidence that the carrier density is not homogeneously distributed in the patterns of competing and coexisting phases. One of the controversial issues in this respect is the scale of these inhomogeneities. While it is widely accepted [6] that non-uniformity is present at the nanoscale level, there are indications of phase separation at the micrometre scale [7].

The compositions with $Mn^{3+}/Mn^{4+} < 1$ are called the electron doped manganites. One end member of this family is the compound $CaMnO_3$, which nominally does not possess Mn^{3+} ions but only Mn^{4+}. At low temperatures, this compound is an insulating anti-ferromagnet of G type. Doping it with trivalent lanthanides leads to rather intriguing changes in the $Ca_{1-x}Ln_xMnO_3$ series [8–12]. At low x values, the substitution of Ca^{2+} for Ln^{3+} is accompanied initially by the rise of the ferromagnetic component in magnetization and increasing conductivity. On further increasing the lanthanide content, the competition between ferromagnetic and anti-ferromagnetic interactions becomes stronger, resulting in peculiar magnetic behaviour of electron manganites. In compositions of the most pronounced colossal magnetoresistance effect, to be referred to hereafter as optimal, namely at $x = 0.13$–0.17, the magnetization exhibits a sharp peaklike anomaly [9]. The peak temperature increases with lanthanide content and decreases with increasing Ln^{3+} ion size. The mixing of different lanthanides substituted into the perovskite structure shifts the optimal x values somewhat and broadens the singularity in the magnetization. At still higher Ln^{3+} content the heavily electron doped manganites reach an anti-ferromagnetic insulating state of C type at low temperatures [12].

The origin of weak ferromagnetism in electron doped manganites was attributed to either canting of predominantly anti-ferromagnetic sublattices or to the presence of ferromagnetic clusters embedded into an anti-ferromagnetic matrix [11–14]. The neutron diffraction studies seem to support the phase separation scenario [15]. The same scenario was used recently to analyse the metastable states in $Ca_{0.85}Sm_{0.15}MnO_3$ [16]. The $x = 0.15$ composition is optimal in the $Ca_{1-x}Sm_xMnO_3$ series [7, 18]. On lowering the temperature, the low field magnetization of $Ca_{0.85}Sm_{0.15}MnO_3$ exhibits a sharp and narrow peak at $T_S = 115$ K, accompanied by a metal–insulator transition. These features are due to the structural transformation from the high temperature orthorhombic $Pnma$ phase, which is paramagnetic, into the low temperature monoclinic $P2_1/m$ phase, which is an anti-ferromagnet of C type. Strong magnetic field causes a collapse of the low temperature phase in $Ca_{0.85}Sm_{0.15}MnO_3$, resulting in a field induced first order transition from the monoclinic anti-ferromagnetic phase to the orthorhombic ferromagnetic phase [16–19]. The $P2_1/m$ phase at low temperatures shows the signatures of phase separation, the ferromagnetic clusters and anti-ferromagnetic clusters of G type being present in an anti-ferromagnetic matrix of C type [18]. The effects of phase separation seem to diminish at higher Ln^{3+} content [12].

We report here on the effects of creating additional disorder at the A-site by a rare earth substitution in electron doped manganites $Ca_{1-x-y}Sm_xNd_yMnO_3$. The various physical measurements carried out on the $Ca_{0.8}Sm_{0.16}Nd_{0.04}MnO_3$ sample point to an enhancement of the phase separation aspect.

2. Samples and experimental set-up

The pellets of manganites $Ca_{1-x-y}Sm_xNd_yMnO_3$ were obtained from the stoichiometric mixture of Sm_2O_3, Nd_2O_3, $CaCO_3$ and MnO_2 by direct solid state synthesis. The mixture

was heated and reground several times by successively raising the sintering temperature from 980 to 1300 °C. The final sintering was done at 1400 °C for 36 h. The resulting product was checked by x-ray diffraction at room temperature showing no measurable traces of the impurity phases in orthorhombic *Pnma* matrix. The magnetization of $Ca_{1-x-y}Sm_xNd_yMnO_3$ pellets, up to 5 T, was measured as a function of temperature (5–300 K) by a Quantum Design SQUID magnetometer. The magnetization measurements in pulsed magnetic field up to 15 T were performed by a standard technique. The magnetic field was obtained by discharging a battery of capacitors on a solenoid. The duration of the pulse was about 10 ms. The magnetization was estimated by an inductive method. The low field ($\sim 10^{-3}$ T) ac magnetic susceptibility was measured in a separate set-up at 70 Hz. The resistivity was obtained by a standard four-probe technique and the same set-up was used to measure the thermal expansion by means of resistive strain gauges attached to the sample. The specific heat was measured by a quasi-adiabatic microcalorimeter.

3. Low field magnetization and ac susceptibility

The temperature dependences of magnetization of $Ca_{1-x-y}Sm_xNd_yMnO_3$ of four different compositions taken during heating in a magnetic field 0.1 T are shown in figure 1. The magnetization of $Ca_{0.85}Sm_{0.08}Nd_{0.07}MnO_3$ and $Ca_{0.85}Sm_{0.10}Nd_{0.05}MnO_3$ samples (in both cases $x + y = 0.15$) exhibits sharp peaks at $T_S \sim 119$ K ($\sim$122 K) and subsequent gradual increase on lowering temperature. The magnetization of $Ca_{0.80}Sm_{0.16}Nd_{0.04}MnO_3$ and $Ca_{0.80}Sm_{0.18}Nd_{0.02}MnO_3$ samples (in both cases $x + y = 0.20$) shows a broader peak at $T_S \sim 162$ K ($\sim$171 K), an abrupt decrease of the moment below this temperature, and a steplike upturn at lower temperatures. The magnitude of magnetization at the peak's temperature in the $(x + y) = 0.15$ samples is somewhat lower than that found in $(x + y) = 0.20$ samples.

The magnetization of the $Ca_{0.80}Sm_{0.16}Nd_{0.04}MnO_3$ sample taken at increasing and decreasing temperature possesses hysteretic features, as shown in figure 2. Most clearly these features are seen in the vicinity of the peak and at the lowest temperatures. There is no appreciable hysteresis at the steplike anomaly. Two anomalies of similar shape are seen at $T_{MI} \sim 109$ K and $T_S \sim 162$ K in the ac magnetic susceptibility, shown in figure 2 (inset). The field dependences of magnetization in the $Ca_{0.80}Sm_{0.16}Nd_{0.04}MnO_3$ sample are linear at high temperatures, as shown in figure 3(a). In a temperature range between the peaklike and steplike anomalies deviations from linearity in the $M(H)$ curves gradually develop, but the weak ferromagnetic component in the magnetization appears only in the vicinity of the steplike upturn (figure 3(b)). The magnetic hysteresis loop taken at $T = 5$ K is shown in figure 3(b) (inset). The slope of the magnetization curves at high field was used to determine the high field magnetic susceptibility shown in figure 4. The temperature dependence of magnetic susceptibility in the high temperature region follows the Curie–Weiss law with a paramagnetic Curie temperature $\Theta \sim 133$ K, indicating a predominance of ferromagnetic interaction in the high temperature phase of this compound. As seen from the inset to figure 4 the spontaneous magnetization at low temperatures is no more than 0.1% of the saturation magnetization $\sim 4\ \mu_B$ for this compound.

4. High field magnetization

The measurements of the magnetization of $Ca_{0.80}Sm_{0.16}Nd_{0.04}MnO_3$ in high magnetic fields show that the application of a magnetic field at low temperatures induces a metamagnetic transition. The field dependences of magnetization of $Ca_{0.80}Sm_{0.16}Nd_{0.04}MnO_3$ taken in a pulsed magnetic field are shown in figure 5. These dependences qualitatively differ on

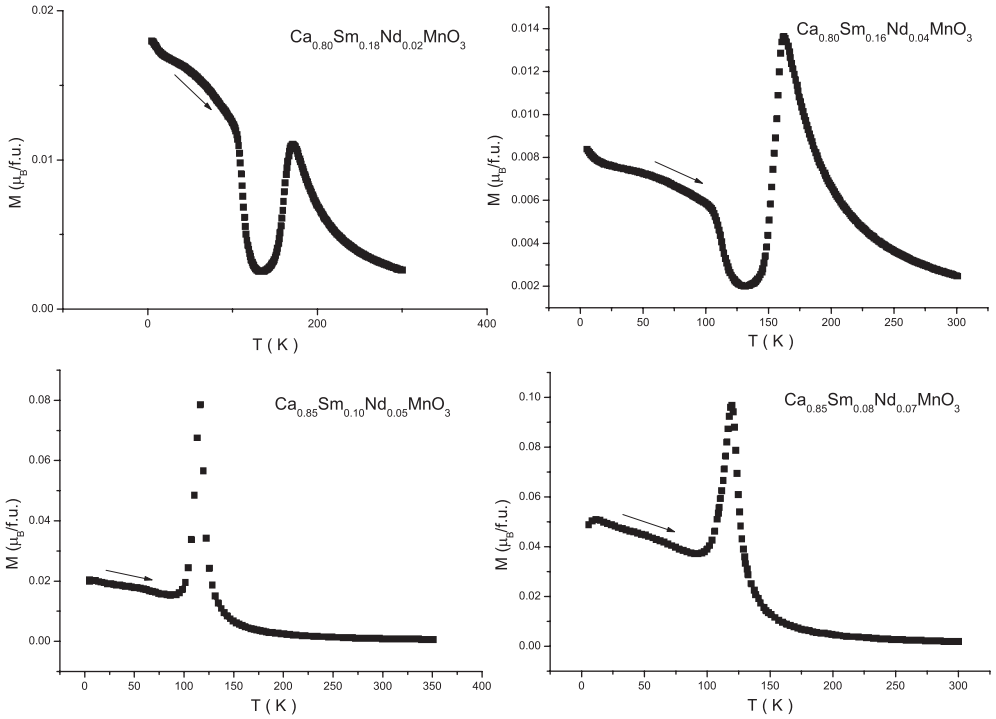

Figure 1. Magnetization as a function of temperature of $Ca_{1-x-y}Sm_xNd_yMnO_3$ of four different compositions in $H = 0.1$ T.

crossing the peak's temperature. Above T_S, the magnetization is almost linear at low fields and experiences the tendency to paramagnetic saturation at high fields. Below T_S, the magnetization is metamagnetic in character and shows the pronounced hysteresis on transition from a low moment state to a high moment state. The critical field of the metamagnetic transition increases on lowering the temperature. At low temperatures the metamagnetic transition is not reached in the magnetic field range studied, so that magnetization just gradually rises on application of magnetic field.

5. Resistivity, thermal expansion and specific heat

The measurements of resistivity, thermal expansion and specific heat were made in the absence of a magnetic field. The resistivity of the $Ca_{0.80}Sm_{0.16}Nd_{0.04}MnO_3$ sample, shown in figure 6, decreases by four orders of magnitude on heating in the range 80–300 K. There are two distinct changes of slope or kinks at $T_{MI} \sim 115$ K and $T_S \sim 158$ K, both leading to a decrease in resistivity. While the kink at T_S separates two different regions of semi-metallic behaviour, that at T_{MI} marks the metal–insulator transition. The thermal expansion of the $Ca_{0.80}Sm_{0.16}Nd_{0.04}MnO_3$ sample, shown in figure 7, is almost linear in the range 80–300 K, except the steplike anomaly $\Delta L/L \sim 10^{-4}$ at $T_S \sim 158$ K. The temperature dependence of the specific heat, shown in figure 8, evidences a well defined peak at $T_S \sim 158$ K while showing no traceable singularities at any other temperature. The area between the experimentally obtained curve and polynomial fitting curve was used to estimate the latent heat of the phase transition, $Q = 610$ J mol^{-1}.

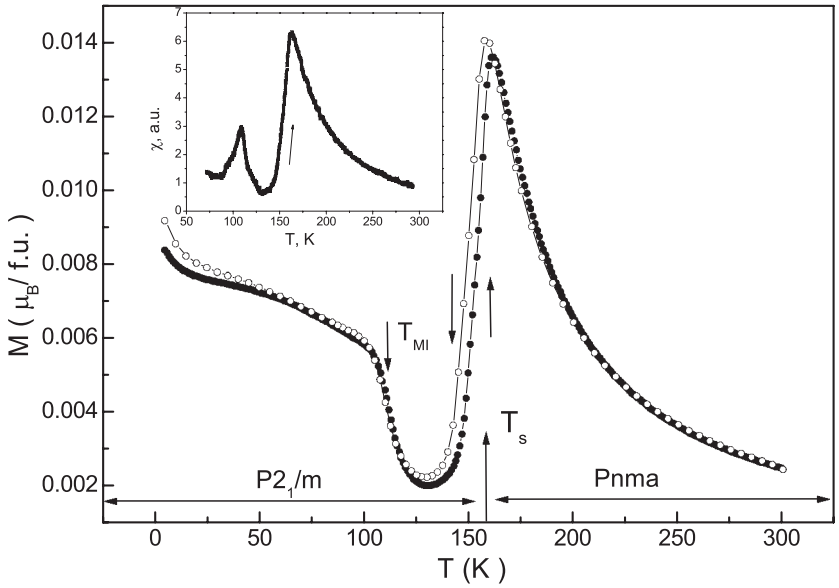

Figure 2. Magnetization as a function of temperature of $Ca_{0.8}Sm_{0.16}Nd_{0.04}MnO_3$ in zero-field cooled (ZFC) and field cooled (FC) regimes. Inset: the temperature dependence of low field ac magnetic susceptibility.

6. Discussion

Based on our experimental data and referring to similar measurements performed on Nd-free $Ca_{1-x}Sm_xMnO_3$ samples [8–10, 17–19], the succession of transitions in $Ca_{0.80}Sm_{0.16}Nd_{0.04}MnO_3$ can be understood as follows. The anomalies of physical properties at $T_S \sim 158 \pm 4$ K in $Ca_{0.80}Sm_{0.16}Nd_{0.04}MnO_3$ are similar to that observed in $Ca_{0.85}Sm_{0.15}MnO_3$ at structural transformation from high temperature orthorhombic $Pnma$ phase to low temperature monoclinic $P2_1/m$ phase. Presumably, a similar transition takes place at complex doping in the present Sm–Nd doped sample. The latent heat of transition in $Ca_{0.80}Sm_{0.16}Nd_{0.04}MnO_3$ is comparable with the latent heat $Q = 500$ J mol^{-1} released [19] during the structural phase transition in $Ca_{0.85}Sm_{0.15}MnO_3$ [19]. The application of high magnetic field at low temperatures results in a field induced structural transformation of first order from monoclinic $P2_1/m$ phase to orthorhombic $Pnma$ phase. This is evident from the metamagnetic character of magnetization curves with a large hysteresis. The specific heat calculated from the jump in magnetization at the metamagnetic transition is in good correspondence with the latent heat released at the spontaneous phase transition.

At $T > T_S$, the sample is paramagnetic and the magnetic susceptibility follows the Curie–Weiss law with paramagnetic Curie temperature $\Theta = 133$ K and effective magnetic moment $\mu_{\text{eff}} \sim 4\ \mu_B$. This value is consistent with the estimate for a given combination of spin only magnetic moments of Sm^{3+}, Nd^{3+}, Mn^{3+} and Mn^{4+} ions in the sample. The predominance of ferromagnetic exchange interaction in the high temperature orthorhombic $Pnma$ phase would lead to the formation of ferromagnetic state in this phase, if the structural transition to anti-ferromagnetic monoclinic $P2_1/m$ phase had not occurred at T_S. The overcooled clusters of $Pnma$ phase are presumably present in the $P2_1/m$ matrix at low temperatures due to the first order character of the structural transformation. Note that ferromagnetic clusters

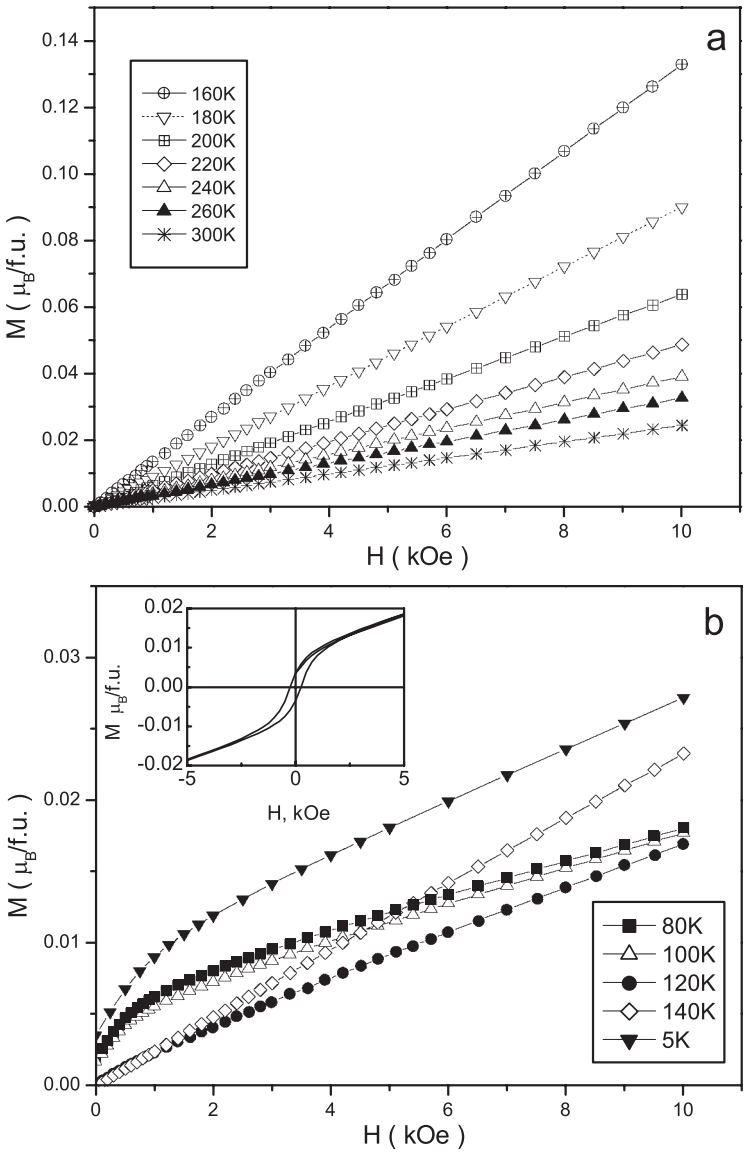

Figure 3. Magnetization as a function of field of $Ca_{0.8}Sm_{0.16}Nd_{0.04}MnO_3$ at $T > T_S$ (panel (a)) and at $T < T_S$ (panel (b)). Inset: the magnetic hysteresis loop at $T = 5$ K.

of orthorhombic phase in antiferromagnetic monoclinic matrix were directly observed in $Sm_{0.15}Ca_{0.85}MnO_3$ [13, 14].

The role played by these clusters is what distinguishes the physical properties of Sm doped from those of the Sm–Nd doped manganites. In $Ca_{0.15}Sm_{0.85}MnO_3$ no other singularities are seen in the physical properties except those in the vicinity of the structural phase transition (cf figure 1 of [17] and figure 1 of the present work). This is because the virtual Curie temperature in this compound practically coincides with the temperature of the structural phase transition. In $Ca_{0.80}Sm_{0.16}Nd_{0.04}MnO_3$ these temperatures are well separated, and this compound experiences an additional phase transition which is due to the ferromagnetic ordering

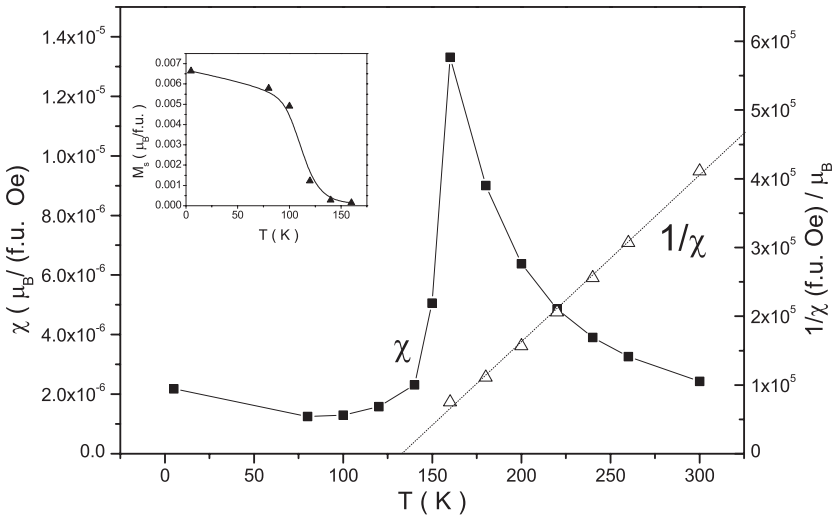

Figure 4. Temperature dependence of susceptibility and inverse paramagnetic susceptibility of $Ca_{0.8}Sm_{0.16}Nd_{0.04}MnO_3$. Inset: temperature dependence of spontaneous magnetization.

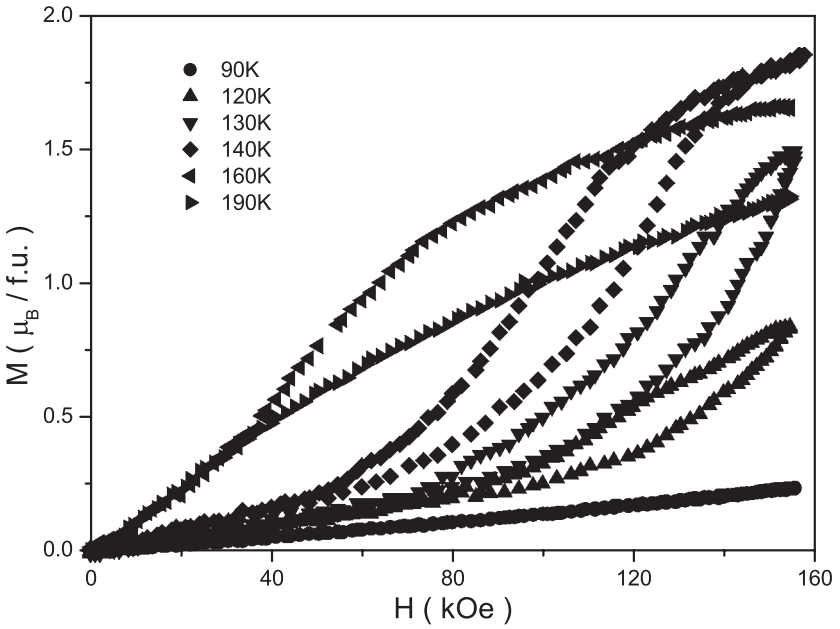

Figure 5. The field dependence of the magnetization of $Ca_{0.8}Sm_{0.16}Nd_{0.04}MnO_3$ taken in a pulsed magnetic field.

in overcooled clusters of orthorhombic phase. It seems that in the more disordered manganites, namely in $Ca_{1-x-y}Sm_xNd_yMnO_3$ samples, the increase in the spread of the size of the doping elements leads to an enhancement of phase separation aspects in resistivity and magnetization measurements.

As shown in figures 2 and 6, the formation of the ferromagnetic state in orthorhombic clusters at T_{MI} is accompanied by the metal–insulator transition. This transition is of special

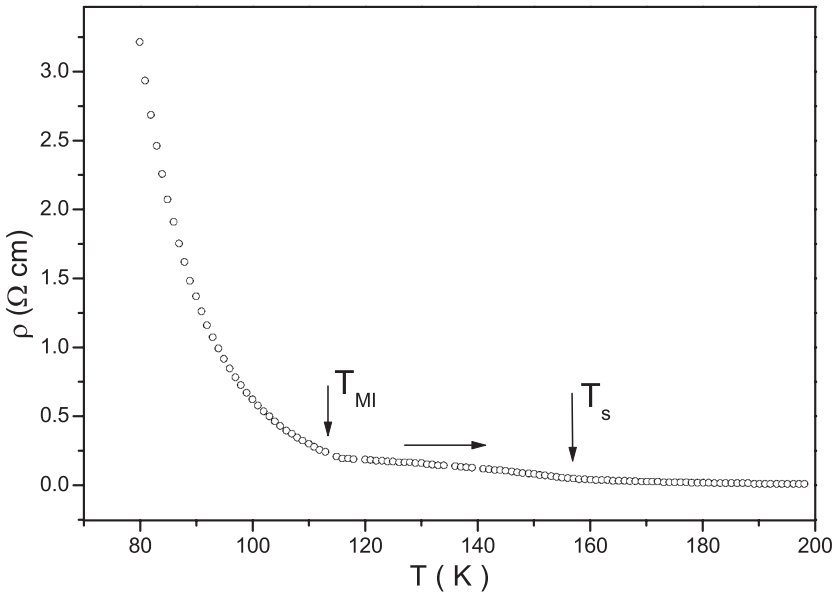

Figure 6. Resistivity of $Ca_{0.8}Sm_{0.16}Nd_{0.04}MnO_3$ as a function of temperature.

importance to get better insight into physical properties of the non-uniform state. One can assume that the ferromagnetic transition in the clusters would not significantly influence the sample's resistivity without the redistribution of carrier density. The ferromagnetic ordering in these clusters is probably accompanied by the 'sponging' of the conduction electrons from the neighbouring anti-ferromagnetic matrix leading the system through the percolation threshold. This process could be favoured by the gain in the kinetic energy of electrons. The absence of anomalies in specific heat and thermal expansion indicates that the ferromagnetic ordering occurs only in minor parts of the sample, not in the matrix itself. These observations once again allow us to exclude the scenario of the transition into a canted anti-ferromagnetic state in the bulk. Otherwise, the appearance of a ferromagnetic component in a basically anti-ferromagnetic matrix would favour the decrease of resistivity. The analytical calculations [20] support the phase separation scenario over that of canted antiferromagnetism.

The size of these clusters in $Ca_{1-x-y}Sm_xNd_yMnO_3$, if any, appears to be an open question. The concept of electronic phase separation at the nanoscale level goes back to early suggestions of ferrons [21], where it was postulated that if two phases have opposite charge, the Coulomb forces break the macroscopic clusters into microscopic ones. While it is not obvious at all that the concept of ferrons is applicable to the manganites discussed here, the experimental observations suggest the presence of large-scale inhomogeneities with percolative and fractal properties [7]. The submicrometre inhomogeneities could not survive once the long-range Coulomb interaction is taken into account. A possible mechanism for the large-scale cluster formation was recently proposed [22]. The essence of this idea is that the neighbouring phases possess different patterns of spontaneous symmetry breaking, so that a transition between them is of first order.

The complex lanthanide doping of electron manganites undoubtedly increases the disorder in the system. Of course, it appears for substitution of Ca by any Ln, since these ions possess different charge. But, even the mismatch effect at doping by isovalent Sm and Nd will lead to additional disorder. In fact, the submicrometre clusters were observed [7] in the compounds

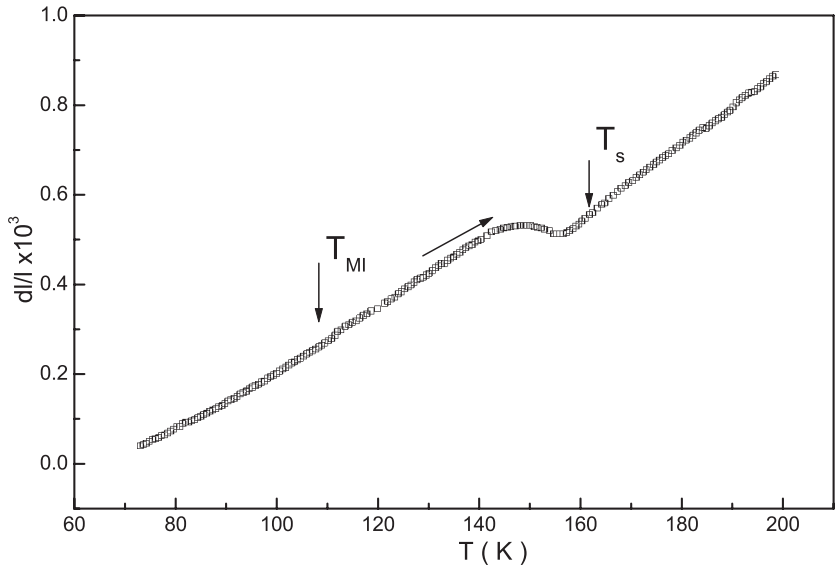

Figure 7. Thermal expansion of $Ca_{0.8}Sm_{0.16}Nd_{0.04}MnO_3$ as a function of temperature.

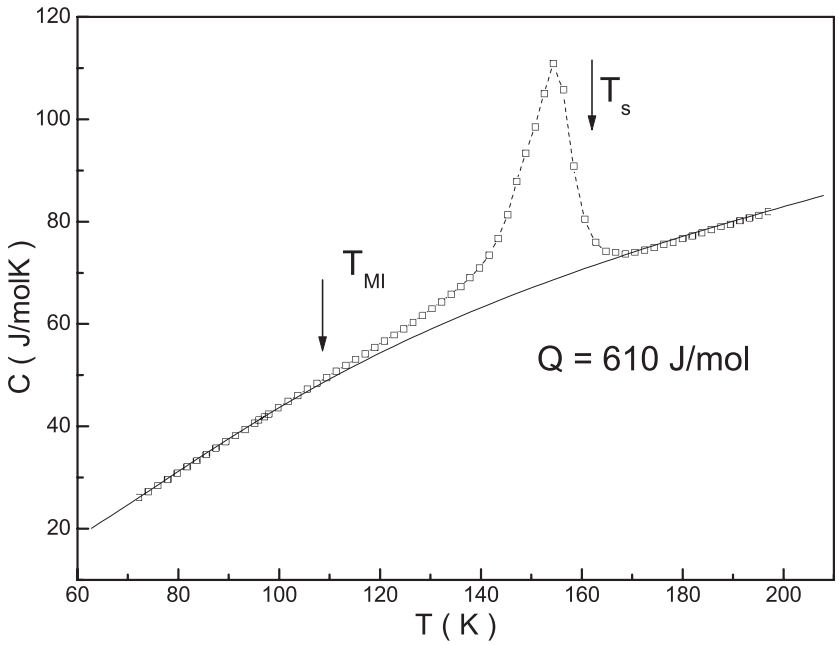

Figure 8. Specific heat of $Ca_{0.8}Sm_{0.16}Nd_{0.04}MnO_3$ as a function of temperature.

with complex lanthanide doping, $(La_{1-y}Pr_y)_{1-x}Ca_xMnO_3$. The Monte Carlo simulations [22] indicate that weak disorder in the vicinity of the first order transition leads to cluster coexistence at a scale much larger than the nanoscale one [6].

7. Conclusion

The experimental data presented here seem to give evidence on the enhancement of various phase separation effects in electron manganites with an increased A-site disorder. The comparison with less disordered samples of the $Ca_{1-x}Sm_xMnO_3$ series allows us to propose that the origin of these effects lies in the increased spread in sizes of trivalent lanthanide cations interpolated into the perovskite structure. The signatures of phase separation appear to be more pronounced in the overdoped $Ca_{0.8}Sm_{0.16}Nd_{0.04}MnO_3$ and $Ca_{0.8}Sm_{0.18}Nd_{0.02}MnO_3$ samples as compared to the optimally doped $Ca_{0.85}Sm_{0.08}Nd_{0.07}MnO_3$ and $Ca_{0.85}Sm_{0.10}Nd_{0.05}MnO_3$ samples. The ground state of $Ca_{0.8}Sm_{0.16}Nd_{0.04}MnO_3$ is assumed to be that of metallic ferromagnetic clusters and insulating anti-ferromagnetic clusters of G type embedded into an insulating anti-ferromagnetic matrix of C type. The metal–insulator transition at $T_{MI} \sim 112 \pm 3$ K occurring well below the structural phase transformation at $T_S \sim 158 \pm 4$ K could be favoured by 'sponging' of carriers by ferromagnetic clusters leaving the matrix insulating. Note that the physical picture outlined above is based on macroscopic measurements, therefore the direct observation of metallic ferromagnetic inclusions on the insulating anti-ferromagnetic background could be of primary importance to check the 'sponging' effect discussed.

The balance between competing phases in electron doped manganites seems to be rather subtle, since small changes in composition lead to large variations in their properties as demonstrated here. The enhancement of the phase separation aspect in complex electron doped manganites should be taken into consideration in fine tuning and optimization of physical properties of colossal magnetoresistance materials. Finally, we would like to point out that the data presented here would be of considerable significance in the light of the recent work by Dagotto [23] wherein the author discusses the relevance of clustered states to the physics of CMR manganites.

Acknowledgments

This work was supported by NWO grant 008-012-047, RFB-BRFBR 02-02-81002, RFBR 02-02-16636 and RFBR 03-02-16108.

References

[1] Rao C N R and Raveau B (ed) 1998 *Colossal Magnetoresistance, Charge Ordering and Related Properties of Manganese Oxides* (Singapore: World Scientific)
[2] Tokura Y (ed) 2000 *Colossal Magnetoresistive Oxides* (New York: Gordon and Breach)
[3] Rodriguez-Martinez L M and Attfield J P 1996 *Phys. Rev.* B **54** R15622
[4] Moreo A, Yunoki S and Dagotto E 1999 *Science* **283** 2034
[5] Salamon M B and Jaime M 2001 *Rev. Mod. Phys.* **73** 583
[6] Dagotto E 2002 *Nanoscale Phase Separation and Colossal Magnetoresistance* (New York: Springer)
[7] Uehara M, Mori S, Chen C H and Cheong S W 1999 *Nature* **399** 560
[8] Maignan A, Martin C, Damay F and Raveau B 1998 *Chem. Mater.* **10** 950
[9] Raveau B, Maignan A, Martin C and Hervieu M 1998 *Chem. Mater.* **10** 2641
[10] Raveau B, Maignan A, Martin C and Hervieu M 1999 *J. Supercond.* **12** 247
[11] Maignan A, Martin C, Damay F, Raveau B and Hejmanek J 1998 *Phys. Rev.* B **58** 2758
[12] Neumeier J J and Cohn J L 2000 *Phys. Rev.* B **61** 14319
[13] Mahendiran R, Maignan A, Martin C, Hervieu M and Raveau B 2000 *Phys. Rev.* B **62** 11644
[14] Martin C, Maignan A, Hervieu M, Raveau B, Jirak Z, Kurbakov A, Trounov V, Andre G and Bouree F 1999 *J. Magn. Magn. Mater.* **205** 184
[15] Respaud M, Broto J M, Rakoto H, Vanacken J, Wagner P, Martin C, Maignan A and Raveau B 2001 *Phys. Rev.* B **63** 14426
[16] Lagutin A S, Vanacken J, Semeno A, Bruynseraede Y and Suryanarayanan R 2003 *Solid State Commun.* **125** 7

[17] Martin C, Maignan A, Damay F, Hervieu M and Raveau B 1997 *J. Solid State Chem.* **134** 198
[18] Algarabel P A, De Teresa J M, García-Landa B, Morellon L, Ibarra M R, Ritter C, Mahendiran R, Maignan A, Hervieu M, Martin C, Raveau B, Kurbakov A and Trounov V 2002 *Phys. Rev.* B **65** 104437
[19] Filippov D A, Levitin R Z, Vasil'ev A N, Voloshok T N, Kageyama H and Suryanarayanan R 2002 *Phys. Rev.* B **65** R100404
[20] Kagan M Yu, Khomskii D I and Mostovoy M V 1999 *Eur. J. Phys.* B **12** 217
[21] Nagaev E L 1967 *JETP Lett.* **6** 18
[22] Moreo A, Mayr M, Feiguin A, Yunoki S and Dagotto E 2000 *Phys. Rev. Lett.* **84** 5568
[23] Dagotto E 2003 *Preprint* cond-mat/0302550